

## Statistical fault diagnosis of wind turbine drivetrain applied to a 5MW floating wind turbine

This content has been downloaded from IOPscience. Please scroll down to see the full text.

2016 J. Phys.: Conf. Ser. 753 052017

(<http://iopscience.iop.org/1742-6596/753/5/052017>)

View [the table of contents for this issue](#), or go to the [journal homepage](#) for more

### Download details:

IP Address: 129.241.221.45

This content was downloaded on 02/11/2016 at 21:50

Please note that [terms and conditions apply](#).

You may also be interested in:

[A new multiscale noise tuning stochastic resonance for enhanced fault diagnosis in wind turbine drivetrains](#)

Bingbing Hu and Bing Li

# Statistical fault diagnosis of wind turbine drivetrain applied to a 5MW floating wind turbine

Mahdi Ghane<sup>1</sup>, Amir R. Nejad<sup>1</sup>, Mogens Blanke<sup>1,2</sup>,  
Zhen Gao<sup>1</sup>, Torgeir Moan<sup>1</sup>

<sup>1</sup>Center for Autonomous Marine Operations and Systems (AMOS), Dept. of Marine Technology and Dept. of Engineering Cybernetics, Norwegian University of Science and Technology (NTNU), NO-7491, Trondheim, Norway

<sup>2</sup>Dept. of Electrical Engineering, Technical University of Denmark (DTU), DK 2800 Kgs. Lyngby, Denmark

E-mail: mahdi.ghane@ntnu.no

**Abstract.** Deployment of large scale wind turbine parks, in particular offshore, requires well organized operation and maintenance strategies to make it as competitive as the classical electric power stations. It is important to ensure systems are safe, profitable, and cost-effective. In this regards, the ability to detect, isolate, estimate, and prognose faults plays an important role. One of the critical wind turbine components is the gearbox. Failures in the gearbox are costly both due to the cost of the gearbox itself and also due to high repair downtime. In order to detect faults as fast as possible to prevent them to develop into failure, statistical change detection is used in this paper. The Cumulative Sum Method (CUSUM) is employed to detect possible defects in the downwind main bearing. A high fidelity gearbox model on a 5-MW spar-type wind turbine is used to generate data for fault-free and faulty conditions of the bearing at the rated wind speed and the associated wave condition. Acceleration measurements are utilized to find residuals used to indirectly detect damages in the bearing. Residuals are found to be non-Gaussian, following a t-distribution with multivariable characteristic parameters. The results in this paper show how the diagnostic scheme can detect change with desired false alarm and detection probabilities.

## 1. Introduction

Wind energy is a rapidly growing renewable energy source, the trend is toward applications further offshore in order to access higher wind and to avoid acoustic noise near populated areas. There are other alternatives to extract offshore energy such as tethered kites [1]. One of the main objectives in any generating asset is to minimize the levelized cost of electricity (LCOE), which is basically computed as the ratio of the total lifetime cost over the total generated energy during the lifetime. LCOE can be minimized by either increasing generated energy or decreasing lifetime costs. Maintenance and repair costs constitute an important portion of the operating costs of a typical wind turbine [2]. These costs are more significant for offshore wind turbines due to limited weather window than onshore ones. Condition monitoring, therefore, offers to play a crucial role in managing the operation and maintenance. Condition monitoring and early detection of incipient degradation following by proper subsystem or supervisory control actions may prevent component failure and system shutdown; moreover, defects could be repaired during planned maintenance, based on condition forecast, a change in concept with a significant savings



potential. Increasing the generated energy by lowering downtime could be another asset of the technology.

A condition monitoring system consists of sensors and data acquisition systems that collect vibration, noise, temperature and strain measurements or oil particle data during a specific period, either online with an integrated measuring system or offline with portable instruments, on a regular basis [3]. Most of the available wind turbine condition monitoring systems are based on existing techniques from other rotating machine industries, see [4] and a review of turbine condition monitoring in [5].

Since it is not possible to monitor all components of a wind turbine, various studies have been conducted to detect the most critical parts. Lu et.al [6] ranked faults according to occurrence and associated downtime, and noted that drivetrain, in particular, the gearbox, is among the most critical subsystems. Moreover, the loadings on drivetrains on floating wind turbines are very different from those are onshore, making the application of condition monitoring particularly attractive. Furthermore, gearbox solutions for offshore development demand higher Reliability, Availability, Maintainability and Serviceability (RAMS) than land-based designs [3]; hence, Fault Detection, Isolation, and Reconfiguration (FDIR) algorithms can be applied to detect components degradation and accommodate them in the shortest possible time.

This paper deals with generation of residuals from the axial acceleration of main shaft which could indicate wear of main shaft bearing in the gearbox and the diagnosis of the degree of wear. In agreement with [7] and [8], the paper shows how residuals could be obtained that are robust to noise and unknown disturbances for the problem at hand. While different techniques are available for analyzing wear in rotating machinery, this paper employ statistical change detection on time-domain signals [9]. Residual generation, which has to be robust to noise and unknown disturbances, as well as various techniques to detect abrupt or gradual change in residual constitute FDI [7]. Different model-based approach in order to generate residual are discussed in Elmatti et al. [8]. Advanced signal processing techniques could be used to analyze the residual in time-domain, frequency-domain and time-frequency domain. Each of them has its own benefits and limitations. Statistical change detection is a well-established method for change detection [9]. The cumulative sum method (CUSUM) is shown to be able to detect fault in down-wind main bearing of a 5MW spar-type wind turbine. The method is shown to be fast and reliable and also to feature estimation of change time which could be useful in estimation the rate of development of wear.

The paper is organized as follows. In Section 2, the functionality of the wind turbine, drivetrain model, and fault scenario are described; detection methodology is explained in Section 3. Next, in Section 4, results and discussion are presented. Conclusions are drawn in Section 5.

## 2. Wind turbine and drivetrain model

A 5 MW reference gearbox [10] installed on the OC3 Hywind floating spar structure [11], [12] is studied in this paper. The wind turbine is a 3-bladed upwind type with rated wind speed of 12.1 m/s. The turbine specification is listed in Table 1.

The spar is a column shaped floating structure which has a large draft and small waterline area. The spar stability is provided by heavy ballast deep in the hull structure [13]. The details of the spar structure, used in this paper, can be found in Nejad et al. [14].

The 5-MW reference gearbox used in this study follows the most conventional design types of those used in wind turbines [10]. The gearbox consists of three stages, two planetary and one parallel stage gears. Table 2 shows the general specifications of this gearbox. Figure 1 shows the gearbox and drivetrain layout. The gearbox topology is also shown in Figure 2. The gearbox was designed with a 4-point support with two main bearings to reduce non-torque loads entering the gearbox.

The multibody system (MBS) model of this gearbox is presented in Figure 3. As it is shown

Table 1: Wind turbine specifications [11], [12].

Parameter	Value
Type	Upwind/3 blades
Cut-in, rated and cut-out wind speed (m/s)	3, 11.4, 25
Hub height (m)	87.6
Rotor diameter (m)	126
Hub diameter (m)	3
Rotor mass ( $\times 1,000$ kg)	110
Nacelle mass ( $\times 1,000$ kg)	240
Hub mass ( $\times 1,000$ kg)	56.8

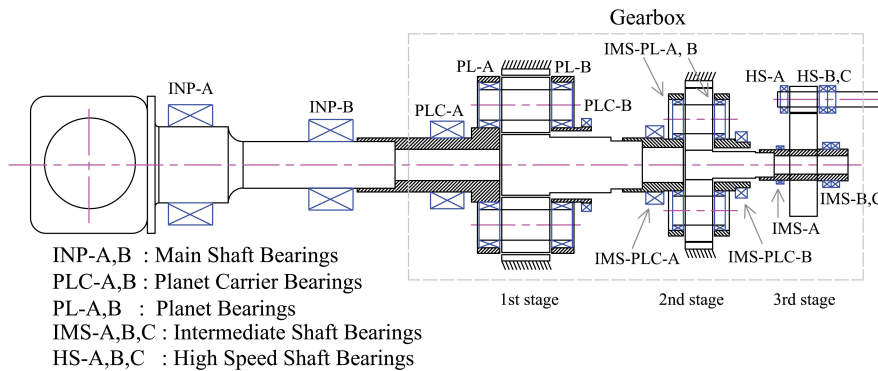


Figure 1: 5-MW reference gearbox layout [10].

Table 2: 5-MW reference gearbox specification [10].

Parameter	Value
Type	2 Planetary + 1 Parallel
1st stage ratio	1:3.947
2nd stage ratio	1:6.167
3rd stage ratio	1:3.958
Total ratio	1:96.354
Designed power (kW)	5000
Rated input shaft speed (rpm)	12.1
Rated generator shaft speed (rpm)	1165.9
Rated input shaft torque (kN.m)	3946
Rated generator shaft torque (kN.m)	40.953
Total dry mass ( $\times 1000$ kg)	53
Service life (year)	20

in the figure, the global motions are applied on the bed plate and the external loads on the main shaft. The generator torque is controlled at the generator side to obtain a desired shaft speed [10].

### 2.1. De-coupled Approach & Environmental Condition

A de-coupled analysis method is employed in this study which is presented in Figure 4, [10]. The procedure is as follows. The forces and moments on the main shaft are first obtained from the global response analysis. The global analysis is conducted by using an aero-hydro-servo-elastic code, SIMO-RIFLEX-AeroDyn [15]. Simulations are carried out at the rated wind speed with wave conditions characterized by significant wave height  $H_S = 5$  m and peak period  $T_P = 12$  s

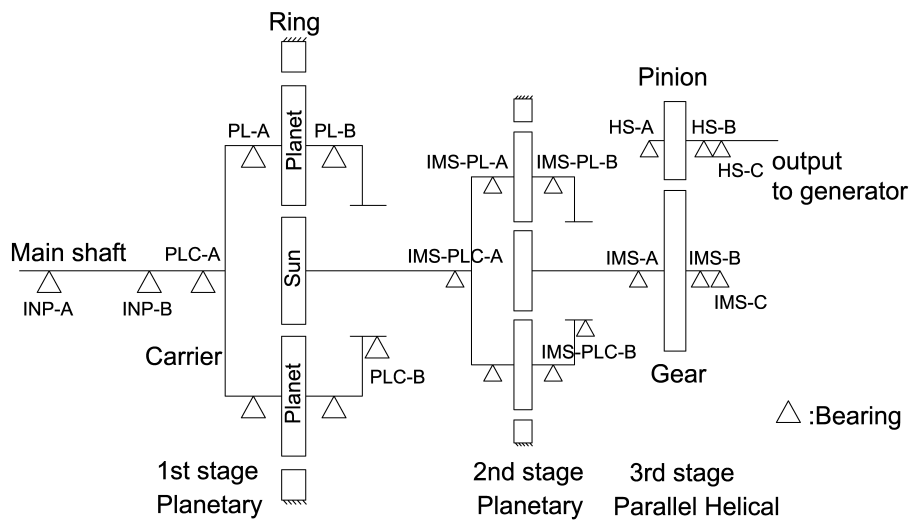


Figure 2: 5-MW reference gearbox topology [10].

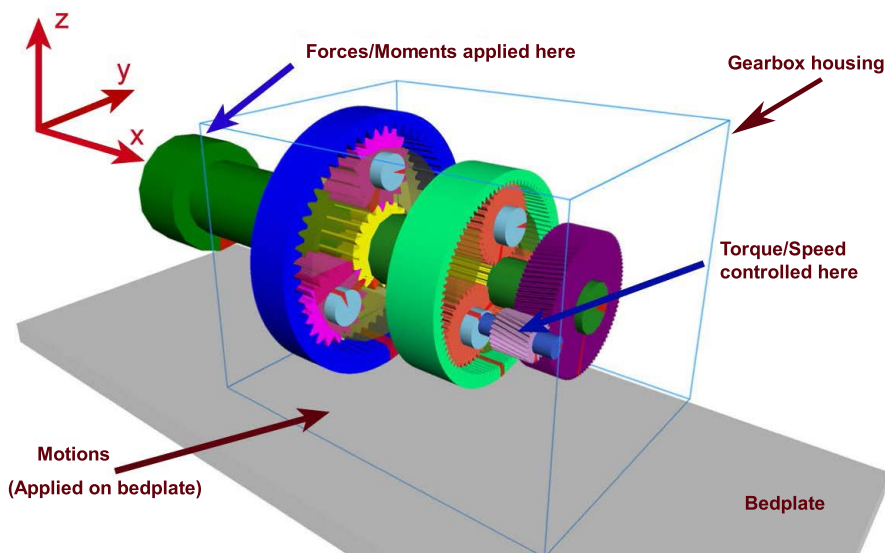


Figure 3: MBS model of the 5-MW reference gearbox [10].

(modelled by a JONSWAP spectrum). The turbulence intensity factor is taken as 0.15 according to IEC 61400-1 [16]. The environmental data used in this study were obtained from a buoy off the coast of Portugal [17]. Simulation over 3800 s was carried out and the first 200 s is removed during post-processing to avoid start-up transient effects.

In the MBS analysis, bearings are modelled as force elements and their force-deflection relation. Gears are modelled with compliance at tooth including detailed tooth properties [10]. The generator model depends on the type of generator. Being widely used in wind turbines, an asynchronous generator with wound rotor is considered in this study. It is simulated by a model that represents both mechanical and electrical characteristics of the generator and the action of the control system. The mechanical equivalent of the model is two inertias coupled by shaft stiffness and damped by control system actions on load torque via magnetizing currents in the rotor. The model replicates both mechanical and electrical properties of the generator and of its

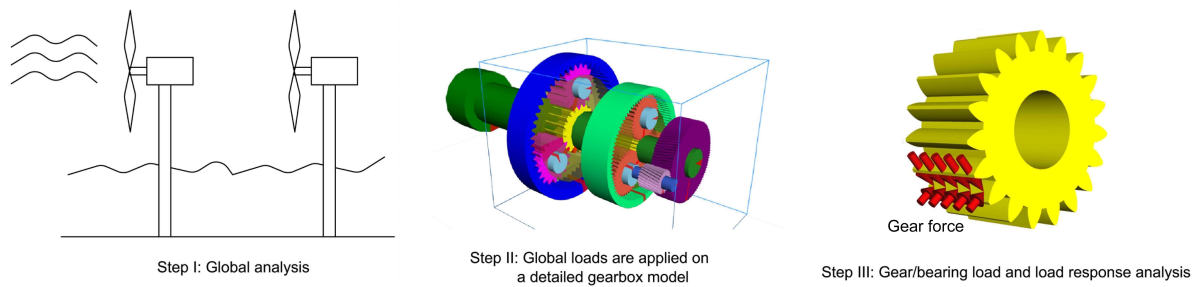


Figure 4: Drivetrain de-coupled analysis method.

control system [18].

### 2.2. Fault Case

The second main bearing (INP-B) in Figure 2, is chosen for the fault study. This bearing in the 5-MW reference gearbox carries the axial load, thus, any damage in this bearing will result transferring axial force to the gearbox. As it has been shown in earlier studies [14], [19] larger axial force than allowed - or non-torque force - has severe effect on lifetime of bearings and gears in the gearbox. The bearing damage is modelled by varying the bearing's deflection [3] in the axial direction. For INP-B, the axial deflection is changed from  $2.5 \times 10^{-3}$  mm to  $2.5 \times 10^{-2}$  mm for each 1 kN applied force, which means bearing stiffness changes from  $400 \text{ KN/mm}$  to  $40 \text{ KN/mm}$ . As it was shown by Qiu et al. [20], there is a direct relation between the bearing stiffness and the damage. Damage in this context means the system damage, considering the bearing as one component. Qiu et al. [20] has shown that the crack propagation and spalling in rollers occurs in a relatively short time after initiation. As a result, there is a fast and considerable change in the bearing stiffness and vibration signals accordingly [21].

The axial force at the INP-B measured in the MBS model is used for the fault detection study. In practice, this force is measured by the acceleration measurement. In the MBS model, the force is calculated from the axial stiffness and the local displacement of the bearing. Damage in the bearing changes its properties and thus affects the deformation and the axial force which can be detected by the reference value known for instance from the MBS model simulation or real measurements [3]. Filtered acceleration of main shaft used in detection algorithm is shown in Figure 5, while sampling frequency is 200 Hz and it is seen that at the middle of the plot fault in bearing happens.

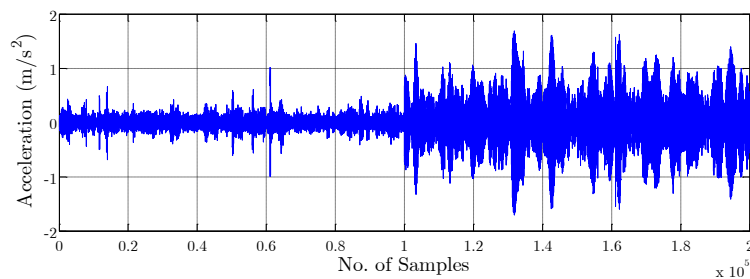


Figure 5: Filtered acceleration of main shaft in x direction

### 3. Change Detection Methodology

Change detection in a linear stochastic continuous/discrete system was addressed by Blanke et al. [9] and Kay [22]. The test presented below will enable us to distinguish between the so called null hypothesis  $H_0$  (no fault is present) and the alternative hypothesis  $H_1$  (a fault is present) using their probability density functions. Consider a sequence of independent random variables  $z(i)$ ,  $i = 1, 2, \dots$ , with probability density function  $p_{\Theta}(z)$  depending upon vector parameter  $\Theta$ . Before an unknown change time,  $k_0$ ,  $\Theta$  is equal to  $\Theta_0$ . At time  $k_0$ , which could be estimated, it changes to  $\Theta = \Theta_1 \neq \Theta_0$ . If there is no prior information on the probability of damage, Neyman-Pearson's approach provide an optimal solution based on likelihood ratio [22]. A log-likelihood ratio test offers an optimal solution which maximize the probability of detection ( $P_D$ ) for a given probability of false alarm ( $P_F$ ), equation 1 and 2.

$$P_F = P(g > h | \mathcal{H}_0) = \int_h^{\infty} p(g | \mathcal{H}_0) dg \quad (1) \quad P_D = P(g > h | \mathcal{H}_1) = \int_h^{\infty} p(g | \mathcal{H}_1) dg \quad (2)$$

Selection of detection threshold  $h$  and a window size of the test are made to meet desired detection properties  $P_F$  and  $P_D$ .

#### 3.1. CUSUM with multivariate t-distribution

A CUSUM algorithm is suited when we wish to detect whether a possible change is above a certain value. Results show that the test statistic in the case considered is not Gaussian, as often assumed in literature [9] and [22], but instead follows a t-distribution with the probability density function as shown in equation 3. In this equation,  $\mu$  is the location parameter representing the distribution center,  $\sigma$  is the scale parameter,  $\nu$  is the shape parameter and  $\Gamma(x)$  is the Gamma function. A univariate generalized likelihood ratio test was derived by Willersrud et al. [23]. The proposed method in this paper is an extension to CUSUM test while data follows a t-distribution with multivariate characteristic parameters.

Given a sequence of  $N$  independent and identically distributed (*IID*) observations of a vector  $\mathbf{z} = \{z(1), \dots, z(k)\}$ . The hypothesis testing problem is to determine most probable hypothesis, from observations  $z(i)$  over a sliding window from current time  $k$  back to  $k - M + 1$  where  $M$  is referred to as the window size equation. 4.

$$f(z(i); \mu, \sigma, \nu) = \frac{\Gamma((1+\nu)/2)}{\Gamma(\frac{\nu}{2})(\pi\nu)^{0.5} \sigma} \times \left[ \frac{\nu + (\frac{z(i)-\mu}{\sigma})^2}{\nu} \right]^{-\frac{1+\nu}{2}} \quad (3)$$

$$\begin{aligned} H_0 : p(z(i)) &\sim t(\mu, \sigma_0, \nu_0) \quad \text{for } k - M + 1 \leq i \leq k \\ H_1 : p(z(i)) &\sim t(\mu, \sigma_1, \nu_1) \quad \text{for } k - M + 1 \leq i \leq k \end{aligned} \quad (4)$$

Since in CUSUM the magnitude of change is assumed to be known, all the parameters of distributions under different hypothesis are known and estimated based on measured data or simulation data. However, the same method could be extended to unknown change and unknown distributions [24]. Test statistics based on log-likelihood ratio is shown in equation 5, where  $M$  is the length of the data sequence used to calculate the test statistic  $g(k)$  at time  $k$ . Estimated distribution's parameters under different hypothesis are shown in Table 3.

$$g(k) = \ln \frac{\prod_{i=k-M+1}^k f(z(i); \mu_1, \sigma_1, \nu_1)}{\prod_{i=k-M+1}^k f(z(i); \mu_0, \sigma_0, \nu_0)} \quad (5)$$

3.2. Thresholds based on CUSUM test statistic approximated by a Weibull distribution

If the CUSUM inputs were Gaussian and IID the distribution of the test statistic  $g(k)$  could be determined analytically which follows a Chi-squared distribution [23]. This allows to make a threshold analytically based on desired probability of detection  $P_D$  and probability of false alarm  $P_F$ . However, in many industrial applications, data often violate these theoretical assumptions. They are neither IID nor Gaussian. Hence, the actual distribution of the test statistic can be very different from the Chi-squared statistics obtained from the theory. One approach to address this issue is to approximate test statistics from experimental data. Accordingly, several distributions were tested and Weibull distribution was found to be a good fit for  $g(k)$ .

4. Results and Discussions

Change in INP-B bearing is modeled as change in stiffness in MBS model. So, acceleration of the main shaft is chosen to detect the degradation. In order to make data, axial acceleration of main shaft, to be robust to the low frequency input disturbances such as wave and wind, axial acceleration was subtracted from nacelle acceleration. The histograms of filtered acceleration data are depicted in Figure 6. Fitted t-distributions, equation 3, are demonstrated in probability plot Figure 7, and Table 3 shows the related parameters for fault-free (Green) and faulty case (Blue).

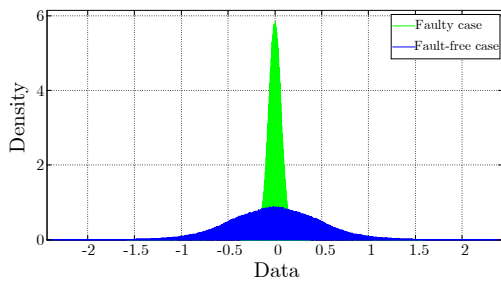


Figure 6: Histogram of acceleration data  $z(i)$

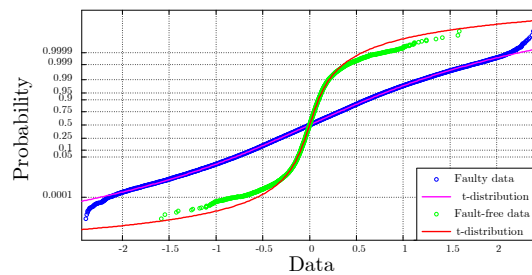


Figure 7: distribution fitting to data

Table 3: Estimated t-distribution parameters for faulty and fault-free cases

	$\mu$ (location)	$\sigma$ (scale parameter)	$\nu$ (shape parameter)
Faulty case	2.62772e-05	0.452984	14.3145
Fault free case	7.90278e-05	0.0639523	5.45911

Simulations were carried out with sampling frequency equal to 200 Hz and for window size  $M = 2400$  samples. Choosing larger  $M$  would result in higher probability of detection and lower probability of false alarm at the expense of slower change detection. Realization of decision function (test statistics) is shown in Figure 8. It is seen that the decision function defers properly before and after fault occurrence resulting in a robust detection. Algorithm set the alarm which is a function of threshold and maximum detection delay, 166 steps after fault occurrence.

Next step is to estimate probability of detection and false alarm for the proposed method. It is too complicated to derive analytically an expression for the test statistics when the data are t-distributed and samples are not independent. Instead, the test statistics,  $g(k)$ , is approximated based on long series of simulation data. This shows that  $g(k)$  can be well approximated by a Weibull distribution. This is illustrated in Figure 10 for data from cases with and without faults. It should be noted that test statistics is right-shifted with a positive DC value to have a wider



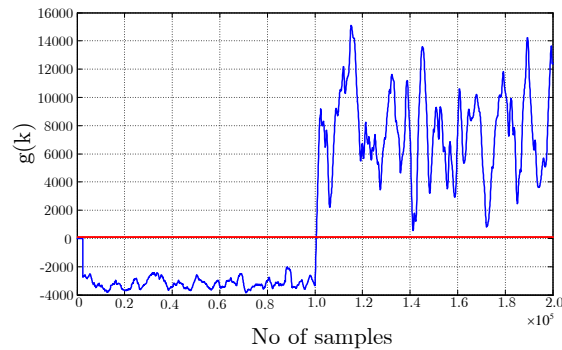


Figure 8: Decision function for M=2400

range of possible distributions to be tested. Weibull distribution and estimated parameters are shown in equation 6 and Table 4. Accordingly, probability of detection and false alarm, equation 1 and 2, are presented in Table 5 for different thresholds.

$$f(x|a, b) = \frac{b}{a} \left(\frac{x}{a}\right)^{b-1} \exp\left\{-\left(\frac{x}{a}\right)^b\right\} \quad (6)$$

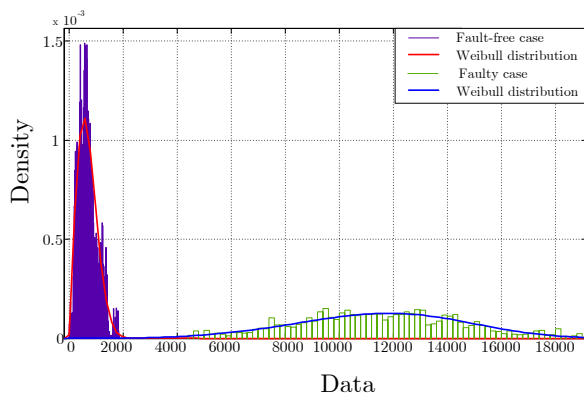


Figure 9: Test statistics histogram

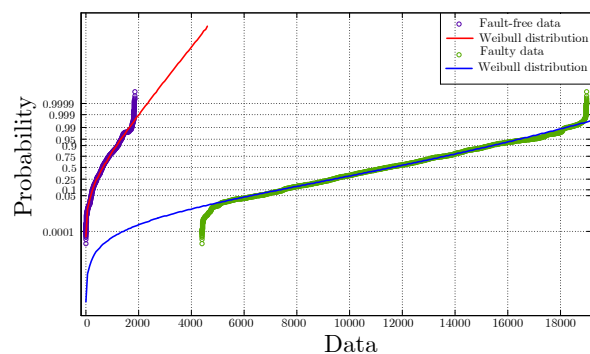


Figure 10: Test statistics distributions

Table 4: Estimated Weibull distribution parameters under different Hypothesis

Hypothesis	$\hat{a}$	$\hat{b}$
Fault-free case( $H_0$ )	771.539	12633.9
Faulty case( $H_1$ )	2.01208	4.18688

Table 5: CUSUM, probability of detection and failure for different threshold

Threshold	Probability of Detection	Probability of false alarm
h=3200	$P_D = 0.9968$	$P_F = 2.51e - 8$
h=4000	$P_D = 0.9919$	$P_F = 1.23e - 12$

Probability of detection and false alarm which are presented in Table 4 are underestimated approximations. It is seen from Figure 10 that test statistics has a sharp roll off under  $H_1$ , such that detection is more sensitive, and therefore  $P_D$  is significantly higher than predicted by the approximating Weibull distribution.

## 5. Conclusion

This paper has demonstrated statistical change detection to t-distributed data from a for wind turbine gearbox and the method was tested on the data from a high fidelity gearbox MBS model of a 5-MW spar wind turbine. The downwind main bearing was chosen for this study due to its high vulnerability. Residuals were distributed according to a central t-distribution and their parameters were estimated for fault free and fault cases in downwind main bearing. A CUSUM algorithm was used to detect a change with known magnitude. Fast detection with a certain probability of detection and false alarm, and capability to detect faults even when fault magnitude is variable with a frequency, not more than the ration of sampling frequency over maximum detection delay are some of the advantageous of the proposed method in comparison to the conventional frequency domain change detection.

## Acknowledgements

The authors wish to acknowledge the financial support from Research Council of Norway through Center for Ships and Ocean Structures (CeSOS) and partially from Centre for Autonomous Marine Operations and Systems (AMOS, project number 223254) at Department of Marine Technology and Department of Engineering Cybernetics, Norwegian University of Science and Technology (NTNU). The second author also thanks Dr. Erin Bachynski from Marine Technology Department for providing the global analysis results of the spar wind turbine.

## References

- [1] Ghasemi A, Olinger D J and Tryggvason G 2015 Computational simulation of the tethered undersea kites for power generation *ASME 2015 International Mechanical Engineering Congress and Exposition* vol 6B (Houston, Texas, USA) pp 43–51
- [2] Poore R and Walford C 2008 Development of an operations and maintenance cost model to identify cost of energy savings for low wind speed turbines Tech. Rep. NREL/SR-500-40581 National Renewable Energy Laboratory (NREL) Midwest Research Institute, Battelle, USA
- [3] Nejad A R, Odgaard P F, Gao Z and Moan T 2014 *Engineering Failure Analysis* **42** 324–336
- [4] Yang W, Tavner P J, Crabtree C J, Feng Y and Qiu Y 2014 *Wind Energy* **17** 673–693 ISSN 1099-1824
- [5] Amirat Y, Benbouzid M E H, Al-Ahmar E, Bensaker B and Turri S 2009 *Renewable and Sustainable Energy Reviews* **13** 2629–2636
- [6] Lu B, Li Y, Wu X and Yang Z 2009 A review of recent advances in wind turbine condition monitoring and fault diagnosis *Power Electronics and Machines in Wind Applications (PEMWA)* (IEEE) pp 1–7
- [7] Hwang I, Kim S, Kim Y and Seah C E 2010 *Control Systems Technology, IEEE Transactions on* **18** 636–653 ISSN 1063-6536
- [8] Ait Elmaati Y, El Bahir L and Faitah K 2015 Residual generation for the gearbox efficiency drop fault detection in the nrel 1.5 windpact turbine *International Conference on Electrical and Information Technologies* (IEEE) pp 77–81
- [9] Blanke M, Kinnaert M, Lunze J and Staroswiecki M 2015 *Diagnosis and Fault-tolerant Control* 3rd ed (Berlin, Heidelberg: Springer-Verlag)
- [10] Nejad A R, Guo Y, Gao Z and Moan T 2015 *Wind Energy* **19** 1089–1106
- [11] Jonkman J M, Butterfield S, Musial W and Scott G 2009 Definition of a 5-mw reference wind turbine for offshore system development Tech. Rep. Technical Report No. NREL/TP-500-38060 National Renewable Energy Laboratory (NREL) Colorado, USA
- [12] Jonkman J M 2010 *Definition of the Floating System for Phase IV of OC3* NREL/TP-500-47535 (Colorado, USA: Citeseer)
- [13] Nejad A, Bachynski E, Gao Z and Moan T 2015 *Procedia Engineering* **101** 330–338
- [14] Nejad A, Bachynski E, Kvittem M, Luan C, Gao Z and Moan T 2015 *Marine Structures* **42** 137–153

- [15] Ormberg H and Bachynski E 2012 Global analysis of floating wind turbines: Code development, model sensitivity and benchmark study *22nd International Ocean and Polar Engineering Conference* vol 1 (Rhodes, Greece) pp 366–373
- [16] 2nd International Electrotechnical Commission 2007 Wind turbines-part 1: Design requirements Tech. rep. IEC-61400-1, Switzerland
- [17] Li L, Gao Z and Moan T 2015 *Journal of Offshore Mechanics and Arctic Engineering* **137** 031901–(1–16)
- [18] E H 2006 *Wind Turbines Fundamentals, Technologies, Application, Economics* 2nd ed (Springer)
- [19] Nejad A R, Xing Y, Guo Y, Keller J, Gao Z and Moan T 2015 *Wind Energy* **18** 2105–2120
- [20] Qiu J, Seth B B, Liang S Y and Zhang C 2002 *Mechanical systems and signal processing* **16** 817–829
- [21] Hoepfich M 1992 *Journal of tribology* **114** 328–333
- [22] Kay S M 1998 *Fundamentals of statistical signal processing: Detection theory, vol. 2* (Upper Saddle River, NJ, USA: Prentice Hall)
- [23] Willersrud A, Blanke M, Imsland L and Pavlov A 2015 *IEEE Transactions on Control Systems Technology*, **23** 1886–1900
- [24] Alippi C and Roveri M 2006 An adaptive cusum-based test for signal change detection *Proceedings of IEEE International Symposium on Circuits and Systems* (Kos, Greek: IEEE) pp 752–755